Asian Journal of Chemistry; Vol. 37, No. 1 (2025), 1-9

ASIAN JOURNAL OF CHEMISTRY

https://doi.org/10.14233/ajchem.2025.32748

Design and Synthesis of Quinazoline Bearing Thiazolotriazole Scaffolds as Potent EGFR Inhibitor for Anti-Breast Cancer Activity

MD FARVEEN[1], G. SREELATHA[1] and ALIA BEGUM[2,*]

[1]Department of Chemistry, Osmania University, Hyderabad-500007, India
[2]Department of Chemistry, Telangana Mahila Viswavidyalayam, Koti, Hyderabad-500095, India

*Corresponding author: E-mail: alia78ou@gmail.com

Received: 22 September 2024; *Accepted*: 8 November 2024; *Published online*: 31 December 2024; AJC-21844

A number of fused heterocyclic hybrids with central rings of thiazolotriazoles are synthesized and characterized by ^{1}H NMR, ^{13}C NMR and EI-MS techniques. The synthesized compounds showed variable degrees of efficacy in their *in vitro* cytotoxic activity against MCF-7, MDA-MB-231 and MCF-10A cell lines. Remarkably some analogues exhibited greater activity than the reference drugs, erlotinib. The most effective compounds, **6i**, **6h** and **6j**, displayed significant EGFR tyrosine kinase inhibition and significant cytotoxicity, in accordance with the molecular docking investigations that revealed favourable binding contacts and energies inside the EGFR active region.

Keywords: Quinazoline, Thiazolotriazole, Breast cancer, EGFR inhibitor, Molecular docking.

INTRODUCTION

As the main cause of cancer related diseases and fatalities for women worldwide, breast cancer demands the development of focused treatment approaches. The epidermal growth factor receptor (EGFR) is a promising target for therapeutic intervention due to its critical role in tumor development, survival and metastasis, among other biological targets [1]. Numerous breast cancer subtypes, particularly those that are resistant to traditional therapies, have been linked to overexpression of EGFR, highlighting the need for new inhibitors with high selectivity and potency [2]. As heterocyclic compounds have a wide range of biological features, they are particularly significant in the medicinal chemistry. Quinazolines, containing an extensive spectrum of biological activities including anticancer [3], antifungal [4], antihypertensive [5], antibacterial [6], antimalarial [7], anticonvulsant [8], anti-inflammatory [9] and anti-HIV [10] activities, are one class of the most significant heterocyclic compounds. The FDA has approved a number of quinazoline moiety based chemotherapy drugs *viz*. erlotinib [10], gefitinib [9] and lapatinib [11]. Furthermore, a number of quinazoline derivatives, including ZM447439 [12], AZD1152 [13], canertinib [14], *etc*. have also been investigated in the clinical studies (Fig. 1).

Thiazolo [3,2-*b*][1,2,4]triazoles are heterocycles with a unique arrangement of nitrogen and sulfur atoms that serve as a scaffold for a variety of modifications that can improve their biological activities [11-13]. Thiazolotriazoles have been shown to exhibit a wide range of medicinal properties, including COX2 inhibition [14], anticancer [15-17], anti-inflammatory [18], antimicrobial [19-22], antidiuretic [14] and analgesic [18] activities. According to recent research, thiazolo[3,2-*b*][1,2,4]-triazole derivatives can interfere with receptor tyrosine kinases, such as EGFR, which is essential for controlling cell growth, survival and differentiation, which demonstrated its strong biological activities [23]. A few examples of molecules consisting thiazolotriazole cores that demonstrate a range of therapeutic uses are shown in Fig. 2.

In order to assess quinazoline bringing thiazolotriazole compounds potential as potent EGFR inhibitors for the treatment of breast cancer, this work focuses on their design, synthesis and characterization. To identify novel compounds with enhanced anti-breast cancer efficacy through a rational drug design approach, thereby providing innovative insights into the therapeutic targeting of the EGFR signaling pathway. The outcomes of this research may pave the way for the innovative treatments which can improve patient outcomes and address the urgent need for more effective breast cancer therapies.

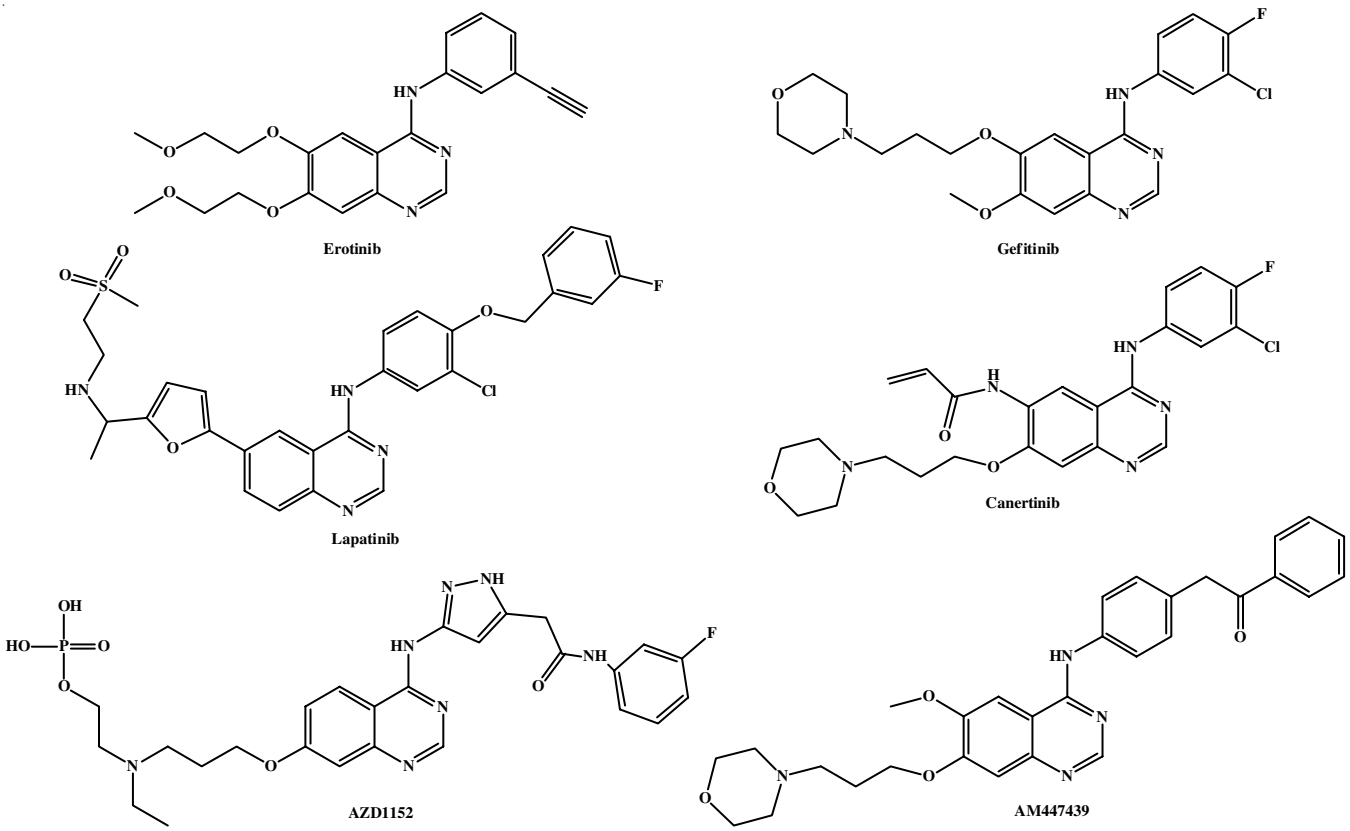

Fig. 1. FDA-approved quinazoline-skeleton chemotherapy drugs

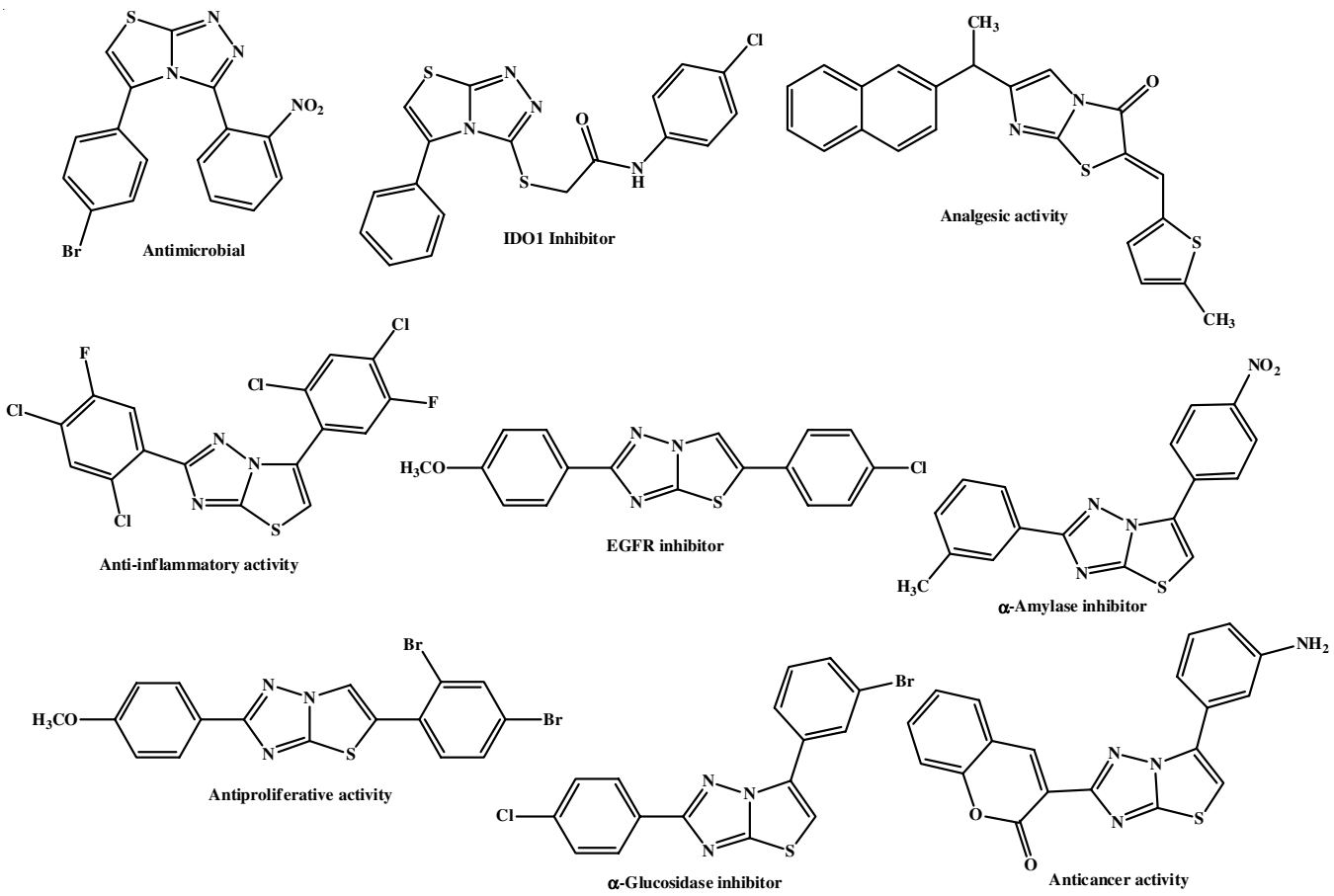

Fig. 2. The thiazolotriazole compounds with biological activities

EXPERIMENTAL

All the reagents were of analytical grade or chemically pure. Analytical TLC was performed on silica gel 60 F_{254} plates. ^{1}H NMR spectra were recorded on a Varian Gemini 400 MHz spectrometer by using TMS as an internal standard. ^{13}C NMR spectra were recorded on a Bruker 100 MHz spectrometer. Mass spectral measurements were conducted using EI method. The elemental analyses were performed on a Carlo Erba 106 and Perkin-Elmer Model 240 analyzers. The melting points were measured with a Cintex apparatus and are not corrected.

2-(Quinazoline-2-carbonyl)hydrazine-1-carbothioamide (3): A mixture containing ethyl quinazoline-2-carboxylate (**1**) (1 mmol, 202 mg) and thiosemicarbazide (**2**) (1 mmol, 91 mg) in 20 mL of methanol was refluxed for 8 h. The product, 2-(quinazoline-2-carbonyl)hydrazine-1-carbothioamide (**3**), was obtained by removing the solvent under reduced pressure, pouring the viscous mass over ice-water, filtered and then recrystallized from a methanol–water mixture (1:1).

5-(Quinazolin-2-yl)-4*H*-1,2,4-triazole-3-thiol (4): 2-(Quinazoline-2-carbonyl)hydrazine-1-carbothioamide (**3**) (1 mmol, 247 mg) dissolved in 15 mL of 8% NaOH solution was heated under reflux for 5 h. After cooling to room temperature, the reaction mixture was acidified with dilute acetic acid, resulting in the precipitate formation. The resulting solid was filtered, washed thoroughly with water and then recrystallized from ethanol to yield 5-(quinazolin-2-yl)-4*H*-1,2,4-triazole-3-thiol (**4**).

6-Phenyl-2-(quinazolin-2-yl)thiazolo[3,2-*b*][1,2,4]-triazole (6a): A solution of 5-(quinazolin-2-yl)-4*H*-1,2,4-triazole-3-thiol (**4**) (1 mmol, 229 mg) and 2-bromo-1-phenylethan-1-one (**5a**) (1.2 mmol, 239 mg) in were mixed in 10 mL of absolute ethanol. The reaction mixture was heated under reflux for 3 h and then cooled to room temperature. Now, added 0.5 mL of conc. H_2SO_4 and refluxed the mixture for additional 3 h, monitoring it with TLC. After cooling, the mixture was poured over ice and neutralized with NaOH solution. The resulting precipitate was filtered and purified column chromatography. The same synthetic procedure was applied with various substituents, to synthesize the similar analogues (**6b-k**) (**Scheme-I**).

6a: White crystalline solid; yield: 84%; m.p.: 148-150 ºC; ^{1}H NMR (400 MHz, DMSO-d_6) δ ppm: 9.50 (s, 1H, quinazoline 4-H), 8.18 (s, 1H, thiazole 5-H), 8.12 (dd, *J* = 7.5, 1.5 Hz, 1H, Ar-H), 7.91 (dt, *J* = 7.5, 1.4 Hz, 1H, Ar-H), 7.84-7.73 (m, 3H, Ar-H), 7.60 (td, *J* = 7.4, 1.4 Hz, 1H, Ar-H), 7.47 (t, *J* = 7.4 Hz, 2H, Ar-H), 7.38 (d, *J* = 7.3 Hz, 1H, Ar-H); ^{13}C NMR (100 MHz, DMSO-d_6) δ ppm: 174.58, 162.55, 159.72, 153.78, 141.37, 140.66, 134.09, 131.00, 129.57, 128.82, 128.04, 127.21, 126.24, 123.61, 112.22; ESI-MS: *m/z* 330.5007 $[M + H]^+$; Calculated, %: $C_{18}H_{11}N_5S$: C, 65.64, H, 3.37, N, 21.26; Found, %: C, 65.69, H, 3.31, N, 21.22.

6-(4-Bromophenyl)-2-(quinazolin-2-yl)thiazolo[3,2-*b*]-[1,2,4]triazole (6b): Light yellow solid; yield 86%; m.p.: 156-158 ºC; ^{1}H NMR (400 MHz, DMSO-d_6) δ ppm: 9.43 (s, 1H, quinazoline 4-H), 8.09 (dd, *J* = 7.4, 1.5 Hz, 1H, Ar-H), 7.87 (dt, *J* = 3.1, 1.3 Hz, 1H, Ar-H), 7.77 (td, *J* = 7.5, 1.5 Hz, 1H, Ar-H), 7.63 (d, *J* = 1.6 Hz, 5H, Ar-H, thiazole 5-H), 7.56 (td, *J* = 7.5, 1.2 Hz, 1H, Ar-H); ^{13}C NMR (100 MHz, DMSO-d_6) δ ppm: 174.55, 162.53, 159.74, 153.75, 141.33, 140.63, 134.08, 132.41, 131.02, 128.29, 128.06, 127.52, 126.26, 123.61, 123.56, 112.25; ESI-MS: *m/z* 408.3000 $[M + 2]^+$; Calculated, %: $C_{18}H_{10}BrN_5S$: C, 52.95, H, 2.47, N, 17.15; Found, %: C, 52.89, H, 2.52, N, 17.19.

2-(Quinazolin-2-yl)-6-(*p*-tolyl)thiazolo[3,2-*b*][1,2,4]-triazole (6c): White crystalline solid; yield: 84%; m.p.: 148-150 ºC; ^{1}H NMR (400 MHz, DMSO-d_6) δ ppm: 9.50 (s, 1H, quinazoline 4-H), 8.18 (s, 1H, thiazole 5-H), 8.12 (dd, *J* = 7.5, 1.5 Hz, 1H, Ar-H), 7.91 (dt, *J* = 7.5, 1.4 Hz, 1H, Ar-H), 7.81 (td, *J* = 7.5, 1.5 Hz, 1H, Ar-H), 7.71 (d, *J* = 7.5 Hz, 2H, Ar-H), 7.60 (td, *J* = 7.4, 1.4 Hz, 1H, Ar-H), 7.34 (d, *J* = 7.5 Hz, 2H, Ar-H), 2.34 (s, 3H, -CH_3); ^{13}C NMR (100 MHz, DMSO-d_6) δ ppm: 174.57, 162.56, 159.73, 153.77, 141.35, 140.65, 138.33, 134.09, 131.03, 130.51, 129.62, 128.07, 127.70, 126.24, 123.63, 112.27, 21.18; ESI-MS: *m/z* 344.3252 $[M + H]^+$; Calculated, %: $C_{19}H_{13}N_5S$: C, 66.45, H, 3.82, N, 20.39; Found, %: C, 66.48, H, 3.78, N, 20.42.

6-(4-Chlorophenyl)-2-(quinazolin-2-yl)thiazolo[3,2-*b*]-[1,2,4]triazole (6d): White crystalline solid; yield: 79%; m.p.: 142-144 ºC; ^{1}H NMR (400 MHz, DMSO-d_6) δ ppm: 9.43 (s, 1H, quinazoline 4-H), 8.09 (dd, *J* = 7.4, 1.4 Hz, 1H, Ar-H), 7.87 (dt, *J* = 3.1, 1.3 Hz, 1H, Ar-H), 7.77 (td, *J* = 7.5, 1.5 Hz,

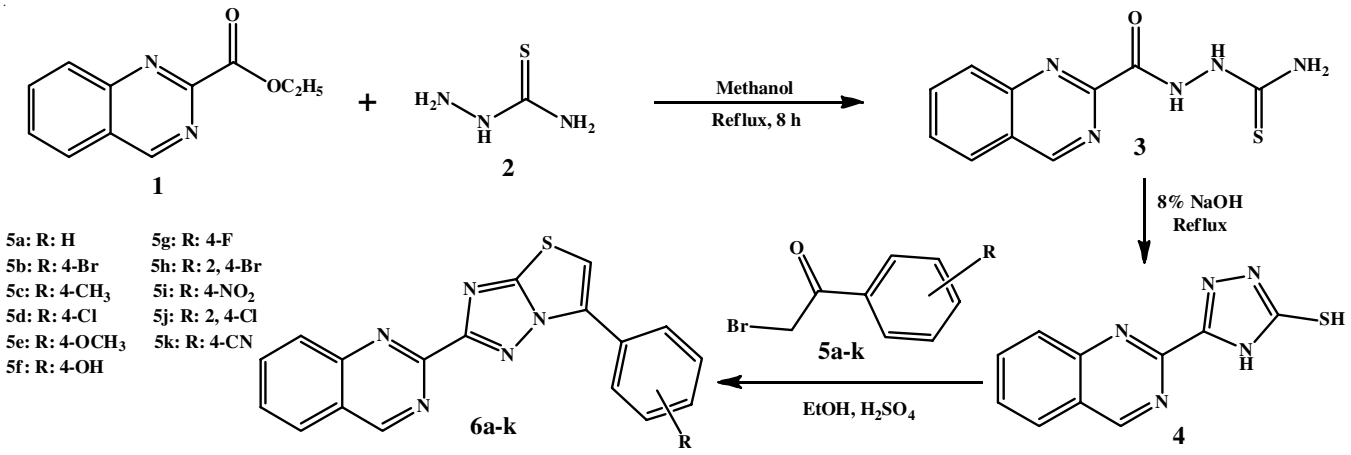

Scheme-I: Synthesis of quinazoline bearing thiazolotriazole Scaffolds

1H, Ar-H), 7.67 (d, *J* = 7.3 Hz, 2H, Ar-H), 7.65 (s, 1H, thiazole 5-H), 7.56 (td, *J* = 7.5, 1.2 Hz, 1H, Ar-H), 7.46 (d, *J* = 7.5 Hz, 2H, Ar-H); ^{13}C NMR (100 MHz, DMSO-d_6) δ ppm: 174.56, 162.52, 159.76, 153.78, 141.37, 140.66, 135.13, 134.05, 132.21, 131.00, 129.30, 129.22, 128.05, 126.28, 123.65, 112.23; ESI-MS: *m/z* 365.0802 $[M + 2]^+$; Calculated, %: $C_{18}H_{10}ClN_5S$: C, 59.42, H, 2.77, N, 19.25; Found, %: C, 59.52, H, 2.82, N, 19.21.

6-(4-Methoxyphenyl)-2-(quinazolin-2-yl)thiazolo[3,2-*b*]-[1,2,4]triazole (6e): Yellow crystalline solid; yield: 80%; m.p.: 156-158 ºC; ^{1}H NMR (400 MHz, DMSO-d_6) δ ppm: 9.48 (s, 1H, quinazoline 4-H), 8.09 (dd, *J* = 7.5, 1.3 Hz, 1H, Ar-H), 7.90 (dt, *J* = 7.5, 1.4 Hz, 1H, Ar-H), 7.79 (td, *J* = 7.4, 1.4 Hz, 1H, Ar-H), 7.67 (d, *J* = 7.5 Hz, 2H, Ar-H), 7.63 (s, 1H, thiazole 5-H), 7.59 (td, *J* = 7.5, 1.4 Hz, 1H, Ar-H), 7.08 (d, *J* = 7.5 Hz, 2H, Ar-H), 3.81 (s, 3H, -OCH_3); ^{13}C NMR (100 MHz, DMSO-d_6) δ ppm: 174.54, 162.57, 159.72, 158.96, 153.75, 141.39, 140.68, 134.04, 131.03, 128.21, 128.06, 126.23, 124.61, 123.62, 115.09, 112.26, 56.06; ESI-MS: *m/z* 360.0660 $[M + H]^+$; Calculated, %: $C_{19}H_{13}N_5OS$: C, 63.50, H, 3.65, N, 19.49; Found, %: C, 63.58, H, 3.61, N, 19.54.

4-(2-(Quinazolin-2-yl)thiazolo[3,2-*b*][1,2,4]triazol-6-yl)phenol (6f): White crystalline solid; yield: 78%; m.p.: 206-208 ºC; ^{1}H NMR (400 MHz, DMSO-d_6) δ ppm: 9.48 (s, 1H, quinazoline 4-H), 8.53 (s, 1H, -OH), 8.12 (dd, *J* = 7.5, 1.2 Hz, 1H, Ar-H), 7.91 (dt, *J* = 7.5, 1.4 Hz, 1H, Ar-H), 7.81 (td, *J* = 7.5, 1.5 Hz, 1H, Ar-H), 7.66 (s, 1H, thiazole 5-H), 7.60 (d, *J* = 7.5 Hz, 3H, Ar-H), 6.97 (d, *J* = 7.5 Hz, 2H, Ar-H); ^{13}C NMR (100 MHz, DMSO-d_6) δ ppm: 174.60, 162.54, 159.76, 159.29, 153.78, 141.37, 140.68, 134.12, 131.09, 128.61, 128.08, 126.36, 123.68, 121.87, 115.75, 112.25; ESI-MS: *m/z* 346.1063 $[M + H]^+$; Calculated, %: $C_{18}H_{11}N_5OS$: C, 62.60, H, 3.21, N, 20.28; Found, %: C, 62.52, H, 3.27, N, 20.35.

6-(4-Fluorophenyl)-2-(quinazolin-2-yl)thiazolo[3,2-*b*]-[1,2,4]triazole (6g): Light brown crystalline solid; yield: 82%; m.p.: 166-168 ºC; ^{1}H NMR (400 MHz, DMSO-d_6) δ ppm: 9.49 (s, 1H, quinazoline 4-H), 8.20 (s, 1H, thiazole), 8.11 (dd, *J* = 7.5, 1.2 Hz, 1H, Ar-H), 7.90 (dt, *J* = 7.5, 1.4 Hz, 1H, Ar-H), 7.80 (td, *J* = 7.5, 1.5 Hz, 1H, Ar-H), 7.73-7.69 (m, 2H, Ar-H), 7.59 (td, *J* = 7.5, 1.5 Hz, 1H, Ar-H), 7.21 (t, *J* = 7.8 Hz, 2H, Ar-H); ^{13}C NMR (100 MHz, DMSO-d_6) δ ppm: 174.56, 162.58, 161.32, 159.78, 153.81, 141.40, 140.63, 134.09, 131.11, 129.73, 128.59, 128.02, 126.28, 123.66, 116.38, 112.28; ESI-MS: *m/z* 347.4803 $[M + H]^+$; Calculated, %: $C_{18}H_{10}FN_5S$: C, 62.24, H, 2.90, N, 20.16; Found, %: C, 62.18, H, 2.96, N, 20.11.

6-(2,4-Dibromophenyl)-2-(quinazolin-2-yl)thiazolo-[3,2-*b*][1,2,4]triazole (6h): Brown crystalline solid; yield: 86%; m.p.: 158-160 ºC; ^{1}H NMR (400 MHz, DMSO-d_6) δ ppm: 9.52 (s, 1H, quinazoline 4-H), 8.21 (s, 1H,, thiazole 5-H), 8.11 (dd, *J* = 7.5, 1.5 Hz, 1H, Ar-H), 7.90 (d, *J* = 7.4 Hz, 1H, Ar-H), 7.88 (s, 1H, Ar-H), 7.80 (td, *J* = 7.5, 1.5 Hz, 1H, Ar-H), 7.63-7.57 (m, 2H, Ar-H), 7.55 (d, *J* = 7.5 Hz, 1H, Ar-H); ^{13}C NMR (100 MHz, DMSO-d_6) δ ppm: 174.62, 162.56, 159.78, 153.75, 141.39, 140.38, 135.77, 134.09, 131.51, 131.00, 129.74, 128.04, 126.24, 123.62, 122.69, 121.56, 109.38; ESI-MS: *m/z* 486.8000 $[M + 2]^+$; Calculated, %: $C_{18}H_9Br_2N_5S$: C, 44.38, H, 1.86, N, 14.38; Found, %: C, 44.42, H, 1.81, N, 14.46.

6-(4-Nitrophenyl)-2-(quinazolin-2-yl)thiazolo[3,2-*b*]-[1,2,4]triazole (6i): Orange crystalline solid; yield: 83%; m.p.: 146-148 ºC; ^{1}H NMR (400 MHz, DMSO-d_6) δ ppm: 9.56 (s, 1H, quinazoline 4-H), 8.39 (d, *J* = 7.5 Hz, 2H, Ar-H), 8.09 (dd, *J* = 7.5, 1.5 Hz, 1H, Ar-H), 7.95 (d, *J* = 7.5 Hz, 2H, Ar-H), 7.90 (dt, *J* = 7.5, 1.3 Hz, 1H, Ar-H), 7.79 (td, *J* = 7.4, 1.4 Hz, 1H, Ar-H), 7.68 (s, 1H, thiazole 5-H), 7.62-7.57 (m, 1H, Ar-H); ^{13}C NMR (100 MHz, DMSO-d_6) δ ppm: 174.63, 162.575, 159.74, 153.79, 147.52, 141.39, 140.65, 135.68, 134.13, 131.09, 128.06, 127.06, 126.24, 125.07, 123.66, 112.29; ESI-MS: *m/z* 375.1062 $[M + H]^+$; Calculated, %: $C_{18}H_{10}N_6O_2S$: C, 57.75, H, 2.69, N, 22.45; Found, %: C, 57.69, H, 2.76, N, 22.53.

6-(2,4-Dichlorophenyl)-2-(quinazolin-2-yl)thiazolo-[3,2-*b*][1,2,4]triazole (6j): White crystalline solid; yield: 83%; m.p.: 154-156 °C; ^{1}H NMR (400 MHz, DMSO-d_6) δ ppm: 9.49 (s, 1H, quinazoline 4-H), 8.15 (s, 1H, thiazole 5-H), 8.11 (dd, *J* = 7.4, 1.4 Hz, 1H, Ar-H), 7.91 (dt, *J* = 3.1, 1.3 Hz, 1H, Ar-H), 7.80 (td, *J* = 7.5, 1.2 Hz, 1H, Ar-H), 7.65 (d, *J* = 7.5 Hz, 1H, Ar-H), 7.60 (td, *J* = 7.5, 1.4 Hz, 1H, Ar-H), 7.56 (s, 1H, Ar-H), 7.39 (dd, *J* = 7.5, 1.5 Hz, 1H, Ar-H); ^{13}C NMR (100 MHz, DMSO-d_6) δ ppm: 174.66, 162.57, 159.73, 153.78, 141.37, 135.13, 134.09, 133.45, 132.95, 131.19, 131.03, 130.25, 128.04, 127.61, 126.24, 124.62, 123.64; ESI-MS: *m/z* 398.9000 $[M + 2]^+$; Calculated, %: $C_{18}H_9Cl_2N_5S$: C, 54.28, H, 2.28, N, 17.29; Found, %: C, 54.36, H, 2.22, N, 17.34.

4-(2-(Quinazolin-2-yl)thiazolo[3,2-*b*][1,2,4]triazol-6-yl)-benzonitrile (6k): Light orange crystalline solid; yield: 86%; m.p.: 162-164 ºC; ^{1}H NMR (400 MHz, DMSO-d_6) δ ppm: 9.59 (s, 1H, quinazoline 4-H), 8.15 (s, 1H, thiazole 5-H), 8.10 (dd, *J* = 7.4, 1.5 Hz, 1H, Ar-H), 7.90 (d, *J* = 7.5 Hz, 3H, Ar-H), 7.80 (td, *J* = 7.5, 1.5 Hz, 1H, Ar-H), 7.73 (d, *J* = 7.5 Hz, 2H, Ar-H), 7.59 (td, *J* = 7.5, 1.5 Hz, 1H, Ar-H); ^{13}C NMR (100 MHz, DMSO-d_6) δ ppm: 174.59, 162.58, 159.77, 153.78, 141.37, 140.67, 134.06, 131.39, 131.01, 130.45, 128.04, 126.28, 123.66, 119.12, 112.82, 112.27; ESI-MS: *m/z* 355.0659 $[M + H]^+$; Calculated, %: $C_{19}H_9N_6S$: C, 64.39, H, 2.84, N, 23.71; Found, %: C, 64.42, H, 2.68, N, 23.66.

RESULTS AND DISCUSSION

The synthesis of 6-phenyl-2-(quinazolin-2-yl)thiazolo-[3,2-*b*][1,2,4]triazole (**6a-k**) scaffolds were made using key intermediate 2-(quinazoline-2-carbonyl)hydrazine-1-carbothioamide (**3**), ethyl quinazoline-2-carboxylate (**1**) and thiosemicarbazide (**2**) were condensed at reflux temperature. The synthesis of 5-(quinazolin-2-yl)-4*H*-1,2,4-triazole-3-thiol (**4**) was obtained by cyclizing 2-(quinazoline-2-carbonyl)-hydrazine-1-carbothioamide (**3**) with 8% NaOH at reflux temperature. After obtaining compound **4**, it was reacted with various α-bromo-4-substituted acetophenones (**5a-k**) with conc. H_2SO_4 subsequently produced the desired 6-phenyl-2-(quinazolin-2-yl)thiazolo[3,2-*b*][1,2,4]triazole scaffolds (**6a-k**).

The newly synthesized structures of analogues **6a-k** were identified using ^{1}H NMR, ^{13}C NMR, ESI mass spectrometry and elemental analysis. In the ^{1}H NMR spectrum of compound **6a**, the singlet proton of quinazoline at 4-H was observed at 9.43 ppm, while the singlet proton of thiazole at 5-H appeared at 8.18 ppm. The cyclized product formation was confirmed

by ^{13}C NMR data, with a signal at 174.58 ppm attributed to the imine (C=N) carbon and a signal at 112.22 ppm corresponding to the thiazolotriazole ring C5 carbon. Additionally, the molecular formula $C_{18}H_{11}N_5S$ was identified, corresponding to a molecular ion peak at *m/z* = 330.05 $[M + H]^+$ in the mass spectrum of compound **6a**.

***In vitro* cytotoxic activity:** The *in vitro* cytotoxicity of newly synthesized thiazolotriazole scaffolds **6a-k** against the cell lines MCF-7 (ATCC-HTB-22), MDA-MB-231 (ATCC-HTB-26) and MCF-10 A (ATCCCRL-10317) was then investigated using the MTT assay [24,25]. Herein, erlotinib was used as a positive control and the results were displayed as IC_{50} with μM. The survival curves for MCF-7 and MDA-MB-231 were generated by plotting the surviving fraction against the drug concentration, as demonstrated in Fig. 3. Based on the cytotoxicity results (Table-1), the analogues had varying degrees of cytotoxicity against the cancer cell lines that were tested. In particular, a compound having a 4-nitrophenyl (**6i**) group on the thiazolotriazole ring showed better cytotoxic activity than erlotinib against two cell lines of breast cancer (IC_{50} values: 3.96 ± 0.09 μM and 6.06 ± 0.05 μM) and a compound comprising 2,4-dibromophenyl (**6h**) on the thiazolotriazole ring demonstrated excellent action against both cell lines with IC_{50} values of 4.19 ± 0.15 μM and 6.22 ± 0.03 μM, respectively. Comparably, compound containing a 2,4-dichlorophenyl (**6j**) on the thiazolotriazole ring demonstrated significantly higher cytotoxic activity against the tested breast cancer cell lines compared to erlotinib. Specifically, it exhibited IC_{50} values of 4.20 ± 0.17 μM for the MCF-7 cell line and 7.13 ± 0.16 μM for the MDA-MB-231 cell line, whereas erlotinib showed IC_{50} values of 4.21 ± 0.43 μM and 7.64 ± 0.04 μM for MCF-7 and MDA-MB-231, respectively.

Compounds **6b**, **6d** and **6k**, which contain 4-bromophenyl, 4-chlorophenyl and 4-cyanophenyl groups, have demonstrated favourable activity against the two cancer cell lines, with IC_{50} values ranging from 6.42 ± 0.53 μM to 13.67 ± 0.26 μM, respectively. Comparing the remaining compounds to the standard drug, they have rather weak performance against both cancer cell lines.

Tyrosine kinase EGFR inhibitory activity: The ability of six active hybrids (**6b**, **6d**, **6h**, **6i**, **6j** and **6k**) to inhibit the tyrosine kinase EGFR using an enzymatic assay, based on their cytotoxic effects [26,27] was investigated. The data in Table-2 demonstrated that compound **6i** was more effective in inhibiting EGFR tyrosine kinase than the positive control, erlotinib (IC_{50} = 0.43 ± 0.05 μM) and the other compounds tested, which had IC_{50} values of 0.39 ± 0.02 μM, respectively. Additionally, compounds **6h** and **6j** displayed equipotent activity compared to regular erlotinib (IC_{50} values of 0.45 ± 0.04 μM and 0.49 ± 0.12 μM). Compounds **6b**, **6d** and **6k** effectively inhibited EGFR; their respective IC_{50} values were 0.83 ± 0.06 μM, 0.68 ± 0.07 μM and 0.64 ± 0.03 μM, respectively.

TABLE-1
In vitro CYTOTOXICITY ACTIVITY WITH IC_{50} (μM)[a]

Compounds	IC_{50} (μM)		
	MCF-7	MDA-MB-231	MCF-10A
6a	23.7 ± 0.19	21.87 ± 0. 13	NT
6b	8.61 ± 0.25	11.44 ± 0.29	16.93 ± 0.13
6c	20.38 ± 0.36	22.88 ± 0.11	NT
6d	11.19 ± 0.18	13.67 ± 0.26	14.32 ± 0.27
6e	25.17 ± 0.08	25.16 ± 0.15	NT
6f	32.85 ± 0.63	28.82 ± 0.08	NT
6g	16.39 ± 0.42	17.53 ± 0.14	NT
6h	4.19 ± 0.15	6.22 ± 0.03	16.42 ± 0.52
6i	3.96 ± 0.09	6.06 ± 0.05	13.53 ± 0.76
6j	4.20 ± 0.17	7.13 ± 0.16	14.12 ± 0.19
6k	6.42 ± 0.53	10.23 ± 0.12	11.35 ± 0.04
Erlotinib	4.21 ± 0.43	7.64 ± 0.04	17.31 ± 0.84

[a]Values are mean ± SD of three replicates. NT = not tested.

TABLE-2
EGFR INHIBITORY ACTIVITY OF POTENT ANALOGUES

Compound	EGFR (IC_{50}, μM)*
6b	0.83 ± 0.06
6d	0.68 ± 0.07
6h	0.45 ± 0.04
6i	0.39 ± 0.02
6j	0.49 ± 0.12
6k	0.64 ± 0.03
Erlotinib	0.43 ± 0.05

*Average of triplicates ± standard deviation.

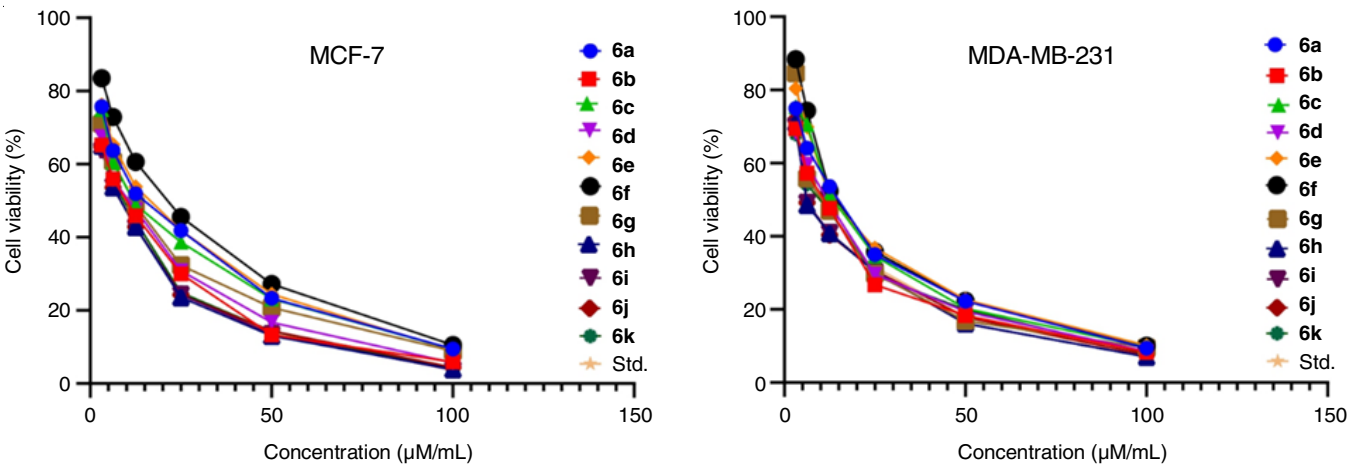

Fig. 3. Survival curves of MCF-7 and MDA-MB231 for thiazolotriazole analogues (**6a-k**)

Molecular docking: One potential strategy for treating cancer is to disrupt the signaling pathway of receptor tyrosine kinases (RTKs), which are often overactivated in cancer [28, 29]. The tyrosine kinase EGFR was selected as the biological target for docking studies on recently synthesized compounds. The crystal structure of the EGFR kinase domain in complex with its inhibitor has been identified (PDB ID: 4HJO) [30]. AutoDock Tools (ADT) version 1.5.6 and AutoDock 4.2.5.1 were used to perform the docking calculations. Erlotinib was docked into the EGFR active site and then replaced it with the synthesized compounds **6a-k** to compare the binding modes of erlotinib and the synthesized compounds.

The crystallized ligand erlotinib inhibitor was shown to exhibit a self-docking process through two hydrogen bond backbone acceptors, Met769 with the quinazoline nitrogen and CYS773 with the methoxy group's oxygen, as shown in Fig. 4. The binding energy of -8.22 Kcal/mol was obtained. The binding energies of all the examined compounds within the active site were found to be between -11.31 and -10.08 Kcal/mol greater than those of erlotinib (Table-3).

Compound **6i** demonstrated three hydrogen bond donors: Asp831 with the nitrogen of the quinazoline moiety, Lys721 with sulfur of thiazole ring and Met769 with oxygen of 4-nitrophenyl moiety, resulting in a binding energy of -11.31 kcal/mol. The docking interactions involved residues of other amino acids including MET742, LEU753, THR766, LEU820, ALA719 and VAL702, respectively (Fig. 5). The second best binding energy score was for compound **6h**, which had one hydrogen bond

TABLE-3
BINDING ENERGY AND HYDROGEN BINDING INTERACTIONS OF COMPOUNDS WITH EGFR KINASE ENZYME INTO THE ACTIVE SITE OF 4HJO

Compounds	Binding energy (kcal/mol)	No. of hydrogen bonds	Residues involved in hydrogen bonding
5a	-10.47	2	LYS721, ASP831
5b	-10.48	2	LYS721, ASP831
5c	-10.08	2	LYS721, ASP831
5d	-10.37	2	LYS721, ASP831
5e	-10.23	2	LYS721, ASP831
5f	-10.16	3	LYS721, ASP831, GLN767
5g	-10.35	3	LYS721, ASP831, MET769
5h	-10.99	1	LYS721
5i	-11.31	3	LYS721, ASP831, MET769
5j	-10.81	1	LYS721
5k	-10.73	3	LYS721, ASP831, MET769
Erlotinib	-8.22	2	MET769, CYS773

with the LYS721 interact with sulfur of thiazole ring and found to be -10.99 Kcal/mol. The linker thiazolotriazole ring exhibited three hydrophobic interactions with LEU834, ASP83 and LYS721, the quinazoline moiety displayed four hydrophobic interactions with MET769, ALA719, LEU820 and GLN767 and the 2,4-dibromophenyl ring shows five hydrophobic interactions with LUE764, PHE832, LEU753, MET742 and VAL745, respectively (Fig. 6). Compound **6j** had a binding energy of -10.81 kcal/mol, where the sulfur atom of the thiazole moiety formed one hydrogen bond with LYS721. The four hydrophobic

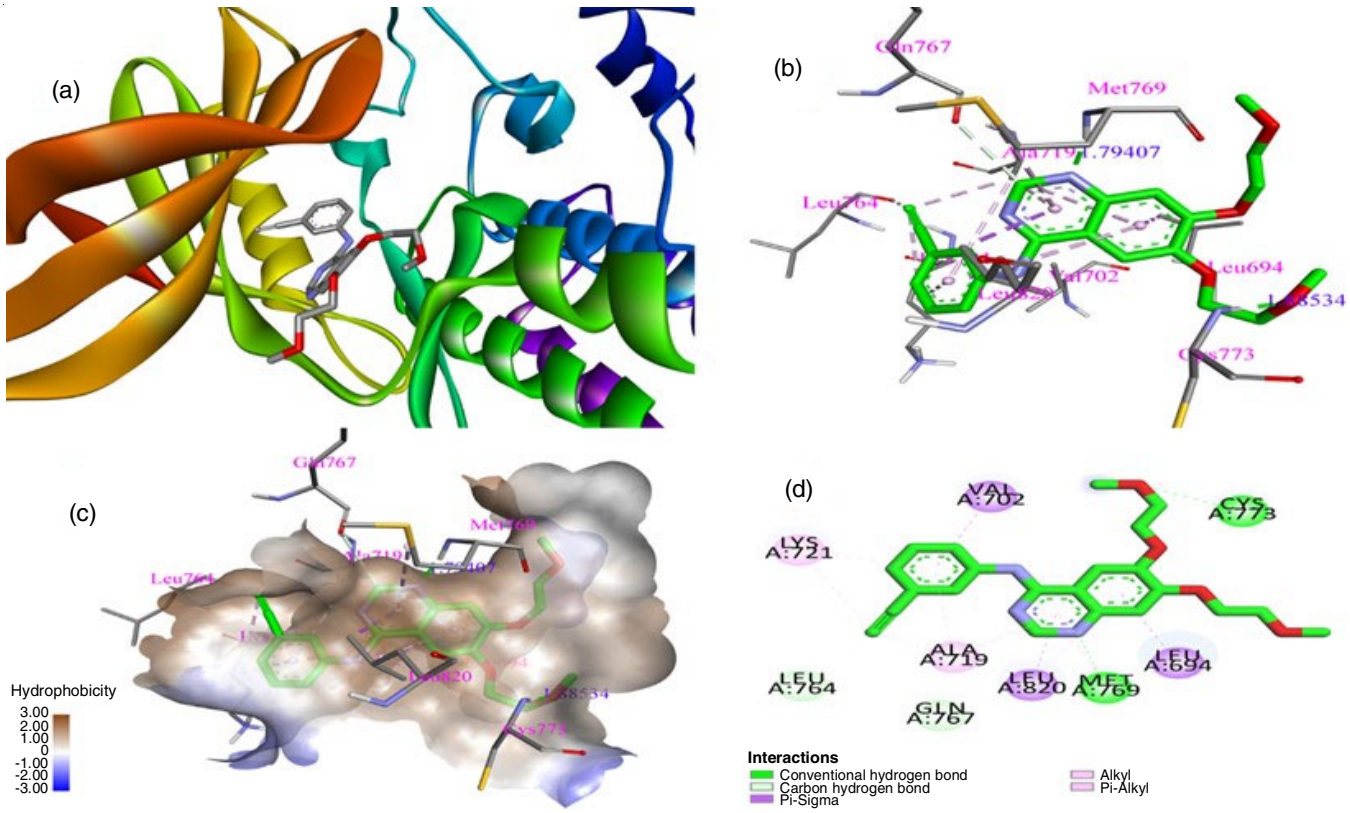

Fig. 4. The binding mode of erlotinib in the active site of EGFR (a) orientation of ligand with protein, (b) 3D interactions, (c) hydrophobic surface interactions, (d) 2D interactions

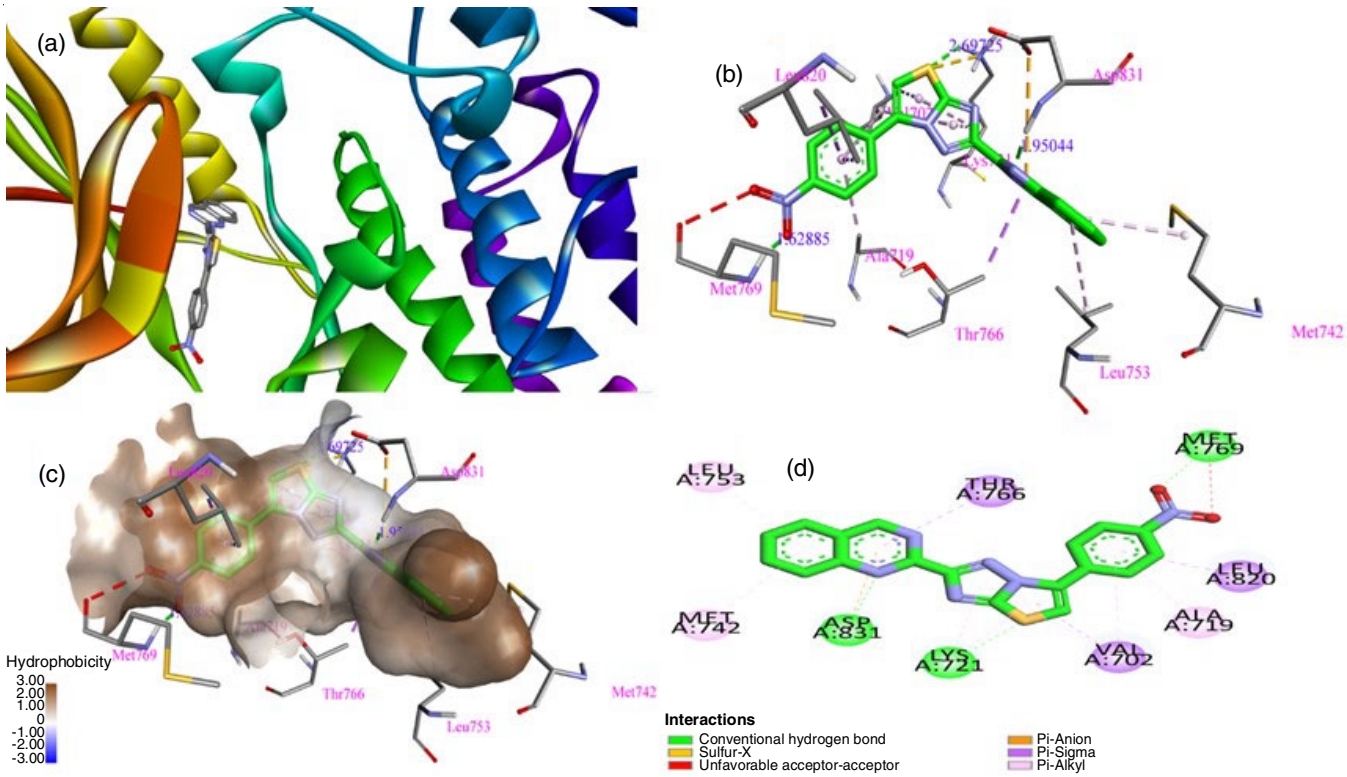

Fig. 5. The binding mode of compound **6i** in the active site of EGFR (a) orientation of ligand with protein, (b) 3D interactions, (c) hydrophobic surface interactions, (d) 2D interactions

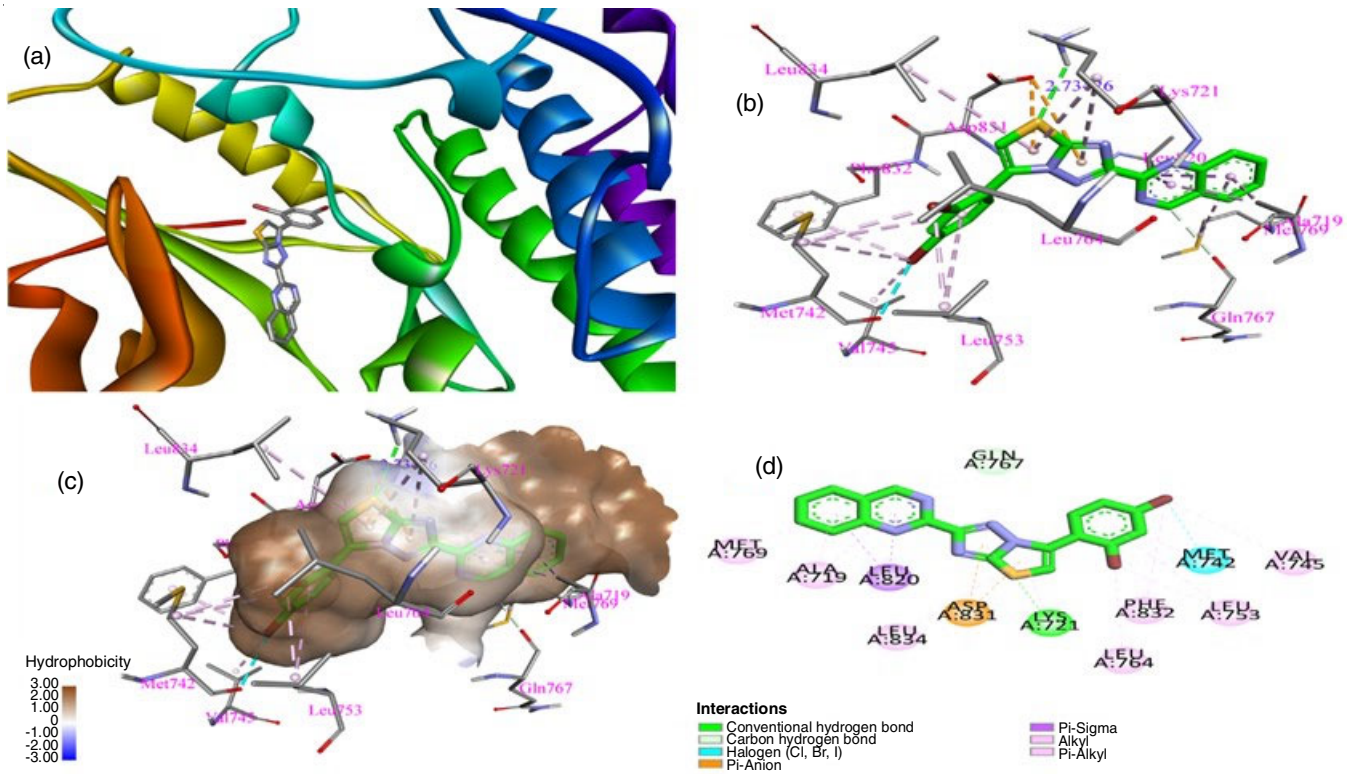

Fig. 6. The binding mode of compound **6h** in the active site of EGFR (a) orientation of ligand with protein, (b) 3D interactions, (c) hydrophobic surface interactions, (d) 2D interactions

interactions with CYS751, MET769, ALA719 and LEU820 generate the quinazoline ring. The thiazolotriazole moiety exhibits the three hydrophobic interactions with ASP831, LYS721 and LEU834. Furthermore, 2,4-dichlorophenyl moiety occupied the formation of five hydrophobic interactions with PHE832, VAL745, MET742, LEU753 and LEU764 (Fig. 7).

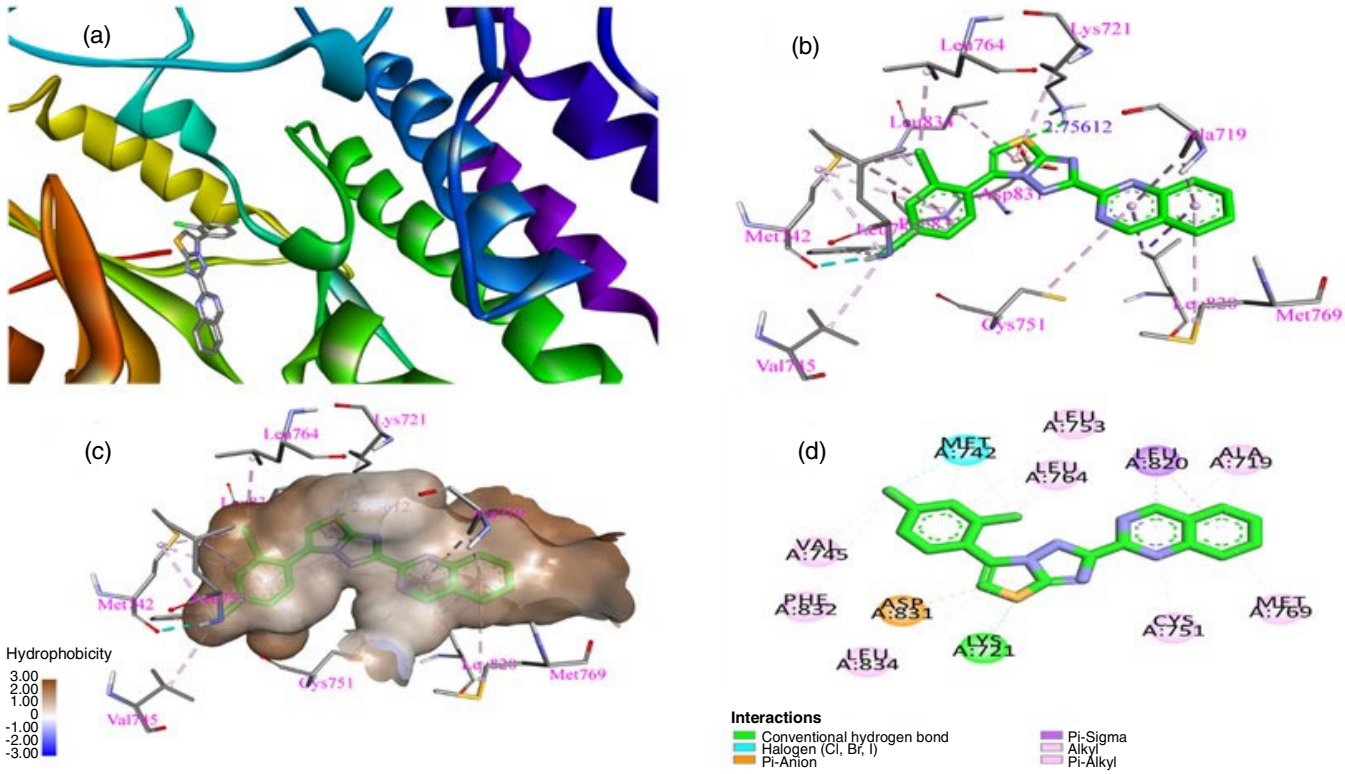

Fig. 7. The binding mode of compound **6j** in the active site of EGFR (a) orientation of ligand with protein, (b) 3D interactions, (c) hydrophobic surface interactions, (d) 2D interactions

Conclusion

The synthesis and biological screening of thiazolotriazole analogues **6a-k** have revealed their potential as effective anticancer agents, particularly against breast cancer cell lines. Compounds having 4-nitrophenyl (**6i**), 2,4-dibromophenyl (**6h**) and 2,4-dichlorophenyl (**6j**) substitutent demonstrated superior cytotoxic activity compared to standard drug, erlotinib. Moreover, these compounds exhibited strong inhibitory activity against EGFR tyrosine kinase, with compound **6i** emerging as the most potent inhibitor. These findings were also confirmed by molecular docking studies, which revealed the favourable binding energies and interactions within the EGFR active site, indicating a potential mechanism of action. The promising results from this study suggest that these newly synthesized thiazolotriazole derivatives could serve as potential leads for the development of novel anticancer therapies, particularly for cancers driven by EGFR signaling.

ACKNOWLEDGEMENTS

The authors are grateful to National Institute of Technology, Warangal, India for providing the NMR, CHN and mass facilities. The authors are also thankful to the Head, Department of Biotechnology and Pharmacy, Kakatiya University, Warangal, India for providing the biological activity.

CONFLICT OF INTEREST

The authors declare that there is no conflict of interests regarding the publication of this article.

REFERENCES

1. G.F.K.P. Zha, H.M. Rakesh, H.M. Manukumar, C.S. Shantharam and S. Long, *Eur. J. Med. Chem.*, **162**, 465 (2019); https://doi.org/10.1016/j.ejmech.2018.11.031
2. Y.G. Zheng, J. Su, C.Y. Gao, P. Jiang, L. An, Y.S. Xue, J. Gao and Y. Liu, *Eur. J. Med. Chem.*, **130**, 393 (2017); https://doi.org/10.1016/j.ejmech.2017.02.061
3. N. Udayasree, R.B. Haridasyam, R. Palabindela, T.M. Krishna and S. Narsimha, *J. Mol. Struct.*, **1320**, 139570 (2025); https://doi.org/10.1016/j.molstruc.2024.139570
4. A.H. Abdelmonsef, M. Omar, H.R. Rashdan, M.M. Taha, A.M. Abobakr, *J. Mol. Struct.*, **1316**, 138854 (2024); https://doi.org/10.1016/j.molstruc.2024.138854
5. M.U. Rahman, A. Rathore, A.A. Siddiqui, G. Parveen and M.S. Yar, *J. Enzyme Inhib. Med. Chem.*, **29**, 733 (2014); https://doi.org/10.3109/14756366.2013.845820
6. A.K. Parhi, Y. Zhang, K.W. Saionz, P. Pradhan, M. Kaul, K. Trivedi, D.S. Pilch and E.J. LaVoie, *Bioorg. Med. Chem. Lett.*, **23**, 4968 (2013); https://doi.org/10.1016/j.bmcl.2013.06.048
7. U.V. Mhetre, N.B. Haval, G.M. Bondle, S.S. Rathod, P.B. Choudhari, J. Kumari, D. Sriram and K.P. Haval, *Bioorg. Med. Chem. Lett.*, **108**, 129800 (2024); https://doi.org/10.1016/j.bmcl.2024.129800
8. H.A. Abuelizz, R.E. Dib, M. Marzouk, E.-H. Anouar, Y. A. Maklad, H. N. Attia and R. Al-Salahi, *Molecules*, **22**, 1094 (2017); https://doi.org/10.3390/molecules22071094
9. M.Z. Luan, X.F. Zhang, Y. Yang, Q.G. Meng and G.G. Hou, *Bioorg. Chem.*, **132**, 106360 (2023); https://doi.org/10.1016/j.bioorg.2023.106360
10. M. Safakish, Z. Hajimahdi, M.R. Aghasadeghi, R. Vahabpour and A. Zarghi, *Curr. HIV Res.*, **18**, 41 (2020); https://doi.org/10.2174/1570162X17666191210105809
11. H. Sachdeva, M. Saquib and K. Tanwar, *Anticancer. Agents Med. Chem.*, **22**, 3269 (2022); https://doi.org/10.2174/1871520622666220412133112

12. N. Seelam, S.P. Shrivastava, S. Prasanthi and S. Gupta, *J. Saudi Chem. Soc.*, **20**, 411 (2016); https://doi.org/10.1016/j.jscs.2012.11.011
13. C. Tratrat, M. Haroun, A. Paparisva, A. Geronikaki, C. Kamoutsis, A. Ciric, J. Glamoèlija, M. Sokovic, C. Fotakis, P. Zoumpoulakis, S.S. Bhunia and A.K. Saxena, *Arab. J. Chem.*, **11**, 573 (2018); https://doi.org/10.1016/j.arabjc.2016.06.007
14. J. Tang, Q. Yi, H. Li, B.J. Kopecky, D. Ding, H.C. Ou, R. DeCook, X. Chen, Z. Sun, M. Kobel and J. Bao, *Hearing Res*., **328**, 59 (2015); https://doi.org/10.1016/j.heares.2015.07.002
15. H.A.M. El-Sherief, B.G.M. Youssif, S.N. Abbas Bukhari, A.H. Abdelazeem, M. Abdel-Aziz and H.M. Abdel-Rahman, *Eur. J. Med. Chem.*, **156**, 774 (2018); https://doi.org/10.1016/j.ejmech.2018.07.024
16. S.A.F. Rostom, M.H. Badr, H.A. Abd El Razik and H.M.A. Ashour, *Eur. J. Med. Chem.*, **139**, 263 (2017); https://doi.org/10.1016/j.ejmech.2017.07.053
17. H.A.M. Gomaa, H.A.M. El-Sherief, S. Hussein, A.M. Gouda, O.I.A. Salem, K.S. Alharbi, A.M. Hayallah and B.G.M. Youssif, *Bioorg. Chem.*, **105**, 104369 (2020); https://doi.org/10.1016/j.bioorg.2020.104369
18. D. Sarigol, A. Uzgoren-Baran, B.C. Tel, E.I. Somuncuoglu, I. Kazkayasi, K. Ozadali-Sari, O. Unsal-Tan, G. Okay, M. Ertan and B. Tozkoparan, *Bioorg. Med. Chem.*, **23**, 2518 (2015); https://doi.org/10.1016/j.bmc.2015.03.049
19. P. Kumar, A. Kumar and J.K. Makrandi, *J. Heterocycl. Chem.*, **50**, 1223 (2013); https://doi.org/10.1002/jhet.1600
20. M.S. Karthikeyan, *Eur. J. Med. Chem.*, **44**, 827 (2009); https://doi.org/10.1016/j.ejmech.2008.04.022
21. M. Kumsi, B. Poojary, P.L. Lobo, N.S. Kumari and A. Chullikana, *Z. Naturforsch. B*, **65**, 1509 (2010); https://doi.org/10.1515/znb-2010-1215
22. T. Krishnaraj and S. Muthusubramanian, *J. Heterocycl. Chem.*, **52**, 1314 (2015); https://doi.org/10.1002/jhet.2161
23. A.E. Maennling, M.K. Tur, M. Niebert, T. Klockenbring, F. Zeppernick, S. Gattenlöhner, I. Meinhold-Heerlein and A.F. Hussain, *Cancers*, **11**, 1826 (2019); https://doi.org/10.3390/cancers11121826
24. N. Udayasree, R.B. Haridasyam, R. Palabindela, T.M. Krishna and S. Narsimha, *J. Mol. Struct.*, **1320**, 139570 (2025); https://doi.org/10.1016/j.molstruc.2024.139570
25. R. Palabindela, R. Bodapati, P. Myadaraveni, G. Ramesh and M. Kasula, *J. Mol. Struct.*, **1317**, 139067 (2024); https://doi.org/10.1016/j.molstruc.2024.139067
26. S. Johnpasha, R. Palabindela, M. Azam, R. Kapavarapu, V. Nasipireddy, S.I. Al-Resayes and S. Narsimha, *J. Mol. Struct.*, **1312**, 138440 (2024); https://doi.org/10.1016/j.molstruc.2024.138440
27. E.R. Sucharitha, S.K. Nukala, N.S. Thirukovela, R. Palabindela, R. Sreerama and S. Narsimha, *ChemistrySelect*, **8**, e202204256 (2023); https://doi.org/10.1002/slct.202204256
28. R. Palabindela, R. Guda, G. Ramesh, P. Myadaraveni, D. Banothu, G. Ravi, R. Korra, H. Mekala and M. Kasula, *J. Heterocycl. Chem.*, **59**, 1533 (2022); https://doi.org/10.1002/jhet.4488
29. S. Amudala, R. Palabindela, S. Bhoomandla, N. Kotilingaiah, J. Sandhya and J. Mandala, *Russ. J. Bioorgan. Chem.*, **50**, 34 (2024); https://doi.org/10.1134/S1068162024010138
30. https://www.rcsb.org/structure/4HJO